University of Pennsylvania
ScholarlyCommons

Departmental Papers (ESE) | Department of Electrical & Systems Engineering

4-24-2000

Design, modeling and preliminary control of a compliant hexapod robot

Uluc Saranli
University of Michigan

Martin Buehler
McGill University

Daniel E. Koditschek
University of Pennsylvania, kod@seas.upenn.edu

Copyright 2000 IEEE. Reprinted from *Proceedings of the IEEE International Conference on Robotics and Automation*, Volume 3, ICRA 2000, pages 2589-2596.

This material is posted here with permission of the IEEE. Such permission of the IEEE does not in any way imply IEEE endorsement of any of the University of Pennsylvania's products or services. Internal or personal use of this material is permitted. However, permission to reprint/republish this material for advertising or promotional purposes or for creating new collective works for resale or redistribution must be obtained from the IEEE by writing to pubs-permissions@ieee.org. By choosing to view this document, you agree to all provisions of the copyright laws protecting it.

NOTE: At the time of publication, author Daniel Koditschek was affiliated with the University of Michigan. Currently, he is a faculty member in the Department of Electrical and Systems Engineering at the University of Pennsylvania.

This paper is posted at ScholarlyCommons. http://repository.upenn.edu/ese_papers/363
For more information, please contact repository@pobox.upenn.edu.

Design, Modeling and Preliminary Control of a Compliant Hexapod Robot

Uluc̣ Saranli[1]*, Martin Buehler[2] and Daniel E. Koditschek[1]

[1]Department of Electrical Engineering and Computer Science
The University of Michigan, Ann Arbor, MI 48109-2110, USA
[2]Center for Intelligent Machines
McGill University, Montreal, QC H3A 2A7, Canada

Abstract

In this paper, we present the design, modeling and preliminary control of RHex, an autonomous dynamically stable hexapod possessing merely six actuated degrees of freedom (at the hip attachment of each leg). Our design emphasizes mechanical simplicity as well as power and computational autonomy, critical components for legged robotics applications. A compliant hexapod model, used to build a simulation environment closely informed the design and construction of the physical machine and promises to inform, similarly, our future analysis as well. Simulations and experiments show that RHex can achieve dynamically stable walking, running and turning with very simple clock driven open-loop control strategies.

1 Introduction

Robotic mobility over highly broken and unstable terrain requires legged machines. Operation within such unstructured settings requires completely self contained power and computation. Survival beyond some fleeting "demonstration" requires a rugged and durable design. But no power and computation autonomous robot has yet been built that is agile enough to run over the lab floor much less offer any service at, say, an earthquake scene. In this paper we report on our first steps toward a machine that we expect will be able to run, walk and hopefully perform rudimentary manipulation within a field of rubble or similar setting that would defy any wheeled or (articulated) tracked vehicle and even a statically balanced legged machine. We describe in some detail a design exercise that has resulted in a working physical prototype hexapod, RHex (http://www.eecs.umich.edu/∼ulucs/rhex/), that presently — following the six week period of its physical construction — runs at roughly one body length (53 cm) per second for roughly fifteen minutes over our laboratory floor with neither power nor computational tether. We sketch in the conclusion the reasons we expect this robot (or, possibly, a more robustly constructed successor) will be able to run considerably faster (perhaps beyond 2 m/s) over badly broken terrain.

Figure 1: *The RHex experimental platform.*

Our design represents what might be considered the minimal configuration for a legged vehicle that leaves room for a reasonably wide range of behaviors. The central obstacle to high performance autonomous machines remains, of course, the very limited power density of contemporary actuation and energy storage technology, and at the most basic level, this design exercise rehearses the familiar tradeoffs between increasing performance and debilitating inefficiency as the number of motors increases. Hexapodal design obviously affords simple low torque solutions to static (parked) and quasi-static (walking) operation, but the commitment as well to the dynamical regime (run-

*Supported in part by DARPA/ONR Grant N00014-98-1-0747

ning) introduces the need for very high joint torques imposed upon rapidly moving limbs. Evidently, once again, the only recourse is to mechanical energy storage: the effective integration of leg springs into our mechanical design represents the chief contribution of this paper. In the conclusion we sketch the manner in which our future controls work with this prototype should transform a design necessity into a performance advantage. As a secondary contribution, an appropriate level of attention to physical modeling details has yielded a sufficiently informative simulation environment, that the construction stage of this prototype proceeded quite rapidly (six weeks) and with very few surprises. Accordingly, we focus a fair bit of attention on these modeling details and the manner in which they have informed our design.

The closest cousins to RHex are arguably the hexapods at Case Western [1, 7, 14] resulting from an outstanding collaboration between neuroscientists, computer scientists and mechanical engineers [2] whose prior work in this area has benefitted us greatly. Their commitment to detailed zoomorphic mimicry results in much greater kinematic complexity (36 degrees of actuated freedom) and the attendant limitations of contemporary commercial actuators incur significant performance limitations. In contrast, our work is informed by specific principles governing animal locomotion (see the conclusion) but our appeal to what might be termed "functional biomimesis" is always subservient to engineering practice. The imperatives of nimble, robust, autonomous operation drive a design which is morphologically alien to any animal and our minimalist orientation affords high performance operation in the dynamical regime with existing commercial technology. A large and growing literature on hexapods initiated by Brooks' Genghis [4] has culminated in a very impressive commercial robot capable of sustained operation in the surf zone [12]. While we aspire to the ruggedness and power autonomy of these designs, they all rely on static or quasi-static balance, while RHex is designed to be a runner. In this regard, our chief inspiration remains the pioneering work of Raibert [15] whose hopping and running machines, although morphologically quite foreign to the present design, inform the future of all dynamically dextrous robotics and represent the real point of departure for our research. The path from Raibert's runners to our RHex leads through the second author's Scout class quadrapeds [5, 6] that reduce mechanical complexity (by the restriction of one actuator per leg) without abandoning dynamical dexterity. In short, the single criterion by which we may best distinguish our machine from the huge surrounding literature is that RHex is designed with the ability to manage its kinetic as well as its potential energy.

2 Design and Modeling

2.1 Design Concept and Morphology

In all robotics applications, mechanical complexity is one of the major sources of failure and considerably increases the cost. Our design emphasizes mechanical simplicity and thereby promotes robustness. Autonomy, a critical component of our aspiration toward real-world tasks in unstructured environments outside the laboratory, imposes very strict design constraints on the hardware and software components. It is often impossible to achieve with simple modifications to a system otherwise designed for non-autonomous operation. These constraints also justify our preference for mechanical simplicity, in particular the minimum amount of actuation and sensing.

Our design depicted in Figure 2 consists of a rigid body with six compliant legs, each possessing only one independently actuated revolute degree of freedom. The attachment points of the legs as well as the joint orientations are all fixed relative to the body and the leg compliance is mainly in the unactuated spherical degrees of freedom.

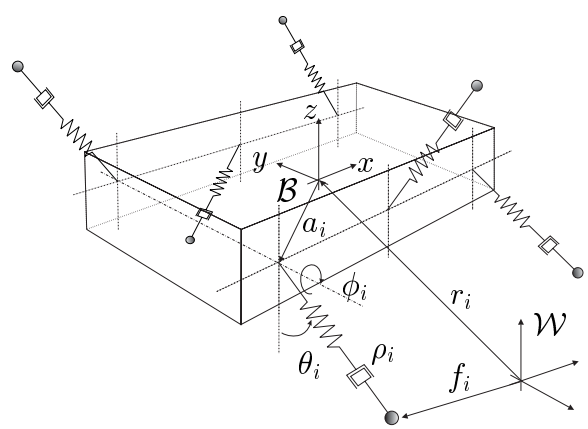

Figure 2: *The Compliant Hexapod Design.*

This configuration admits an alternating tripod gait for forward and backward locomotion, as well as other more elaborate (yet to be achieved) behaviors such as leaping, stair climbing etc. Moreover, the symmetry of the design allows identical upside-down operation and imposes no restrictions on forward directionality. We explore some of this behavioral repertoire both in simulation and experimentally in Section 4 and Section 5, respectively.

States	
$\mathbf{r_b}$, $\mathbf{R_b}$	body position and orientation
$\dot{\mathbf{r}}_\mathbf{b}$	translational velocity of body
$\mathbf{w_b}$	angular velocity of body
Leg states and parameters	
$\mathbf{a_i}$	leg attachment point in $\mathcal{B}$
$\mathbf{f_i}$	toe position in $\mathcal{W}$
$\mathbf{v_i}$	$:= [\theta_i, \phi_i, \rho_i]^T$ leg state in spherical coordinates
$\overline{\mathbf{v}}_\mathbf{i}$	leg state in cartesian coordinates
leg_i	stance flag for leg i
Forces and Torques	
F_{r_i}	radial leg spring force
τ_{θ_i}	bend torque in θ_i direction
τ_{ϕ_i}	hip torque in ϕ_i direction
System Parameters	
M_0	inertia matrix in $\mathcal{B}$
M	inertia matrix in $\mathcal{W}$
m	body mass
Controller Parameters	
$\mathbf{u}$	$:= [t_c, t_s, \phi_s, \phi_o]$ control vector
t_c	period of rotation for a single leg
t_s	duration of slow leg swing
ϕ_s	leg sweep angle for slow leg swing
ϕ_o	leg angle offset

Table 1: Notation used throughout the paper

2.2 The Compliant Hexapod Model

Two reference frames, $\mathcal{B}$ and $\mathcal{W}$ are defined in Figure 2, the former attached to the hexapod body and the latter an inertial frame where the dynamics are formulated. The position and orientation of the rigid body are described by $\mathbf{r_b} \in R^3$ and $\mathbf{R_b} \in SO(3)$, respectively, expressed in $\mathcal{W}$. Table 1 details the notation used throughout the paper.

Each leg is assumed to be massless and has complete spherical freedom. The leg state is described in the spherical coordinate frame $[\theta_i, \phi_i, \rho_i]^T$ whose origin is located at $\mathbf{a_i}$ in the body frame. Note that $(\mathbf{r_b}, \mathbf{R_b})$, $\mathbf{v_i}$ and $\mathbf{f_i}$ are related through a simple coordinate transformation.

2.2.1 Analysis of a Single Leg

Our formulation of the equations of motion for the hexapod model is based on individually incorporating the ground reaction forces at each leg. To this end, it will suffice to analyze a generic leg parametrized by its attachment and touchdown points, $\mathbf{a_i}$ and $\mathbf{f_i}$, respectively, (see Figure 3). The force and torque balance on the massless leg result in the following equalities.

$$\begin{aligned} F_1 &= F_{r_i} \\ F_2 &= \frac{\tau_{\theta_i}}{\rho_i} \\ F_3 &= \frac{\tau_{\phi_i}}{\rho_i \cos\theta_i}. \end{aligned}$$

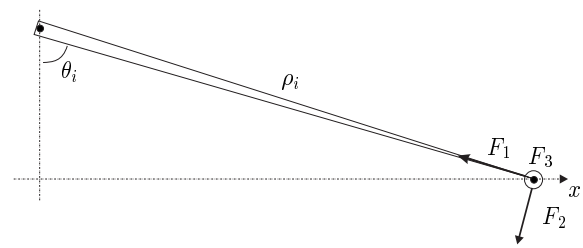

Figure 3: *Analysis of a single leg in the plane defined by the leg and the y-axis of $\mathcal{B}$.*

The body experiences the negative of the ground reaction force on the leg, resulting in an effective force and torque vectors acting on the center of mass. After projections to $\mathcal{B}$, for each leg $i = 1, ..., 6$ we have,

$$\begin{aligned} \mathbf{F_i} &= \begin{bmatrix} -\cos\theta_i \sin\phi_i & \sin\theta_i \sin\phi_i & -\cos\phi_i \\ \sin\theta_i & \cos\theta_i & 0 \\ \cos\theta_i \cos\phi_i & -\sin\theta_i \cos\phi_i & -\sin\phi_i \end{bmatrix} \cdot \\ &\qquad \begin{bmatrix} F_{r_i} \\ \tau_{\theta_i}/\rho_i \\ \tau_{\phi_i}/(\rho_i \cos\theta_i) \end{bmatrix} \\ \tau_\mathbf{i} &= (\overline{\mathbf{v}}_\mathbf{i} + \mathbf{a_i}) \times \mathbf{F_i} \end{aligned}$$

which are the force and torque contributions of a single leg to the overall system dynamics.

2.2.2 Equations of Motion

The cumulative effect of all the legs on the body is simply the sum of the individual contributions, together with the gravitational force. Note that the legs which are not in contact with the ground have no effect on the body. The force and torque vectors, expressed in $\mathcal{W}$, are hence given by

$$\mathbf{F_T} = \begin{bmatrix} 0 \\ 0 \\ -mg \end{bmatrix} + \mathbf{R_b} \sum_{i=1}^{6} leg_i \mathbf{F_i} \tag{1}$$

$$\tau_\mathbf{T} = \mathbf{R_b} \sum_{i=1}^{6} leg_i \tau_\mathbf{i} \tag{2}$$

$$leg_i := \begin{cases} 0 & \textit{leg i is in flight} \\ 1 & \textit{leg i is in stance} \end{cases}$$

The dynamics of a rigid body under this external force and torque actuation is governed by the following equations [10].

$$\begin{aligned} \ddot{\mathbf{r}}_{\mathbf{b}} &= \frac{\mathbf{F_T}}{m} \\ M\dot{\mathbf{w}}_{\mathbf{b}} &= -J(\mathbf{w_b})M\mathbf{w_b} + \tau_{\mathbf{T}} \\ \dot{\mathbf{R}}_{\mathbf{b}} &= J(\mathbf{w_b})\mathbf{R_b} \end{aligned}$$

where we have

$$\begin{aligned} J(\begin{bmatrix} w_x & w_y & w_z \end{bmatrix}^T) &:= \begin{bmatrix} 0 & -w_z & w_y \\ w_z & 0 & -w_x \\ -w_y & w_x & 0 \end{bmatrix} \\ M &:= \mathbf{R_b} M_0 \mathbf{R_b}^{-1} \end{aligned}$$

3 Preliminary Control Strategy

In our initial simulations as well as the experiments on the compliant hexapod robot, we have used joint space closed loop ("proprioceptive") but task space open loop control strategies. The algorithms that we describe in this section are tailored to demonstrate the intrinsic stability properties of the compliant hexapod morphology and emphasize its ability to operate without a sensor-rich environment. Specifically, we present a 4-parameter family of controllers, that yields stable running and turning of the hexapod on flat terrain, without explicit enforcement of quasi-static stability.

Both controllers generate clock driven desired trajectories for each hip joint, which are then tracked by PD controllers for each individual hip joint. As such, they represent examples near one extreme of possible control strategies, ranging from purely clock driven controllers to control laws which are solely functions of rigid body state. It is evident that neither one of these extremes is the best approach and a combination of these should be adopted. The simulations and experiments presented in this paper attempt to characterize the properties associated with the clock driven approach, which we then hope to complement with feedback to explore the aforementioned range.

An alternating tripod pattern governs both the running and turning controllers, where the legs forming the left and right tripods are synchronized with each other and are 180° out of phase with the opposite tripod.

3.1 Running

The running controller's target trajectories for each tripod are periodic functions of time, parametrized by four variables: t_c, t_s, ϕ_s and ϕ_o. The period of both profiles is t_c. In conjunction with t_s, it determines the duty factor of each tripod. In a single cycle, both tripods go through their slow and fast swing phases, covering ϕ_s and $2\pi - \phi_s$ of the complete rotation, respectively. The duration of double support t_d (where all six legs are in contact with the ground) is determined by the duty factors of both tripods. Finally, the ϕ_o parameter offsets the motion profile with respect to the vertical (see Figure 4). Note that both profiles are monotonically increasing in time; but they can be negated to obtain backward running.

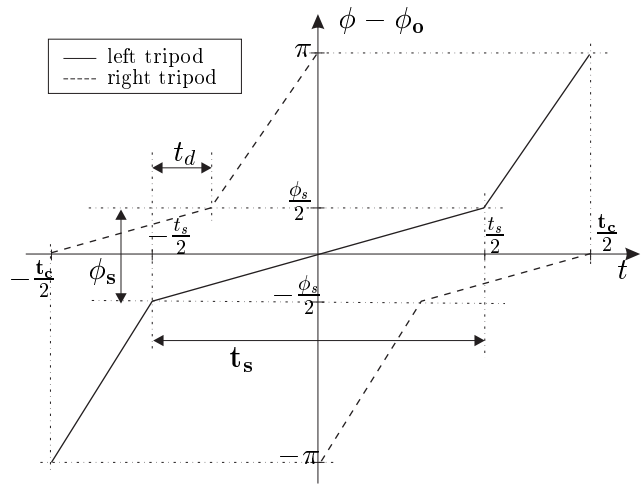

Figure 4: *The motion profiles for left and right tripods.*

Control of running behavior is achieved by modifying these parameters for a particular desired behavior during locomotion. In Section 4, our simulation studies reveal correlations of these parameters with certain attributes of running behavior. We demonstrate that control of average forward running velocity under actuation and power constraints is possible with these controller outputs.

3.2 Turning In Place

The controller for turning in place employs the same leg profiles as for running except that contralateral sets of legs rotate in opposite directions. This results in the hexapod turning in place in the direction determined by the rotational polarity of the left and right sets of legs. Note that the tripods are still synchronized internally, maintaining three supporting legs on the ground. Similar to the control of the forward locomotion speed, the rate of turning depends on the choice of the particular motion parameters, mainly t_c and ϕ_s.

4 Simulation Studies

4.1 Actuator Model

In simulating the compliant hexapod, we also incorporate a simple model of the hip actuation. This model imposes realistic limitations on the torque capabilities of the actuators and, together with the battery model of the following section provides a means of estimating the power consumption of the overall system.

Figure 5(a) portrays the torque-speed curve for the DC motors in the experimental platform. In addition to these torque limits, the model also incorporates an estimation loop for motor voltages v_i and currents i_i using the commanded leg torques, under the assumption that the electrical dynamics are negligible relative to the mechanical dynamics. In consequence, we have

$$\begin{aligned} i_i &= \tau_{\phi_i}/(K_\tau k_g) \\ v_i &= i_i r_a + K_w w_{\phi_i}/k_g \end{aligned}$$

where K_τ and K_w are motor constants, k_g is the gear reduction ratio of 33:1 at the motor shaft and r_a is the motor armature resistance. Note that in this simple formulation, the only influence of the actuator model on the mechanical dynamics is through the limits on the maximum available torque.

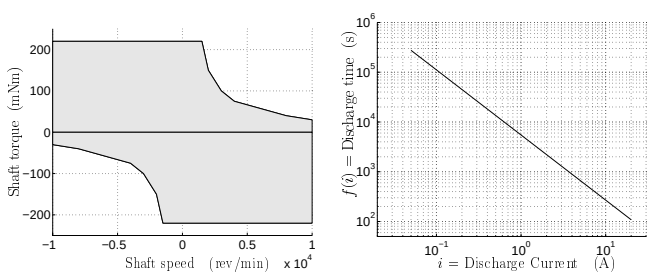

(a) (b)

Figure 5: *(a) Torque-speed curve for the Maxon RE118751 20W DC motor. (b) Battery discharge curve for the Panasonic 12 V, 2.2 Ah battery.*

4.2 Battery Model

The discharge characteristics of off-the-shelf small batteries are usually given by plots of discharge time vs constant discharge current. Figure 5(b) is such a discharge curve for the battery used in our experimental platform. In our discharge model, we use this curve, together with an approximation of the PWM electronics driving the DC motors to estimate the duration of autonomous operation.

First, we derive a method for estimating battery discharge in terms of a continuous time function of varying discharge current. This can be accomplished with

$$\frac{dC(t)}{dt} = -\frac{1}{f(i_a(t))}$$

where $C(t)$ is the percent "energy" left in the battery, and $f(i)$ is the battery discharge curve in functional form. During the hexapod operation, all six motors draw current and contribute to the battery discharge together. Due to the H-bridge output stages of the motor drives, the motor currents add up, yielding the battery lifetime equation

$$1 - \int_0^t \frac{d\sigma}{f(\sum_{i=1}^{6} |i_i(\sigma)|)} = 0.$$

Our battery model detects in simulation the zero crossing of this function, which yields the effective lifetime of the battery. Note that this model does not take into account more elaborate components such as the battery voltage drop as a function of current and discharge time or the effects of ambient temperature.

4.3 Simulation Environment

All the simulation results of the next section are produced by *SimSect*, a custom simulation environment that we have created primarily for the study of the compliant hexapod platform. It provides a generic means of integrating the equations of motion for hybrid dynamical systems with configurable accurate discrete event detection and a 4th order Runge-Kutta integrator [16].

The hexapod simulation with *SimSect* uses the same dimensions and body mass as our experimental platform (see Section 5). However, some of the dynamical parameters used in the simulations, including the leg spring and damping constants, the body inertia matrix and the ground friction coefficient are not experimentally verified and are likely to be different from their actual values. Nevertheless, because our simulations and robotic platform have the same morphology and mass, we will still be able to do qualitative comparisons of behavior.

4.4 Simulation Results

In this section, we verify in simulation that the controllers of Section 3 are able to produce stable autonomous running and turning of the hexapod platform. We first present simulations with the running controller, followed by turning studies. Finally, we use the battery model of Section 4.2 to estimate the duration of operation of the platform.

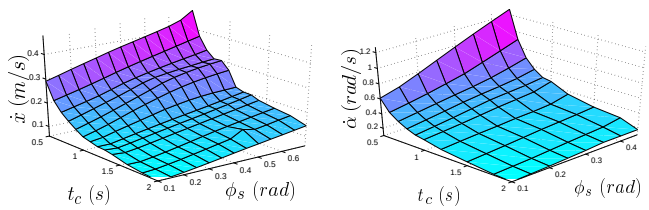

(a) (b)

Figure 6: *(a) Average forward running velocity $\dot{x}$ as a function of t_c and ϕ_s over 5s of operation. Remaining controller parameters are chosen as $t_s = t_c/2$, $\phi_o = 0$. (b) Average in-place turning yaw rate $\dot{\alpha}$ as a function of t_c and ϕ_s over 5s of operation. Remaining controller parameters are chosen as $t_s = t_c/2$, $\phi_o = 0$.*

Figure 6(a) shows the the forward running velocity as a function of controller parameters t_c and ϕ_s. Note that for these simulations, the remaining two parameters, t_s and ϕ_o, have been kept constant.

Similar to the forward running controller, the turning controller also presents a controllable range of turning speeds. Figure 6(b) shows the average angular body velocity as a function of the controller parameters.

Finally, in Figure 7, we present the predicted lifetime of the on-board battery as a function of controller parameters. Our model predicts continuous autonomous running with the low-end Panasonic 12 V 2.2 Ah off-the shelf battery for up to 20 minutes, depending on the particular choice of controller parameters. An important detail which is not immediately visible from the graphs is that different controller parameters yielding the same speed, result in different battery lifetimes. This freedom of choice in the controller parameters, given a particular speed, can be used for optimizing the battery lifetime, as well as other measures such as the maximum motor torque to avoid overheating.

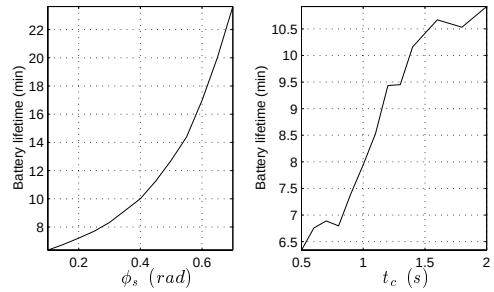

Figure 7: *The battery lifetime a) as a function of t_c with $\phi_s = 0.15rad$ kept constant. b) as a function of ϕ_s with $t_c = 0.6s$ kept constant.*

5 Experimental Platform

5.1 Hardware Description

We have built an experimental platform as an instantiation of the design concepts of Section 2.1. RHex is an autonomous hexapod robot with compliant legs, very close to the model described in Section 2.2. All the computational and motor control hardware is on board, together with two 12 V 2.2 Ah sealed lead-acid batteries for power autonomous operation. A PC104 stack with a 100 MHz Intel 486 microprocessor, together with several I/O boards performs all the necessary computation and implements the controllers of Section 3. A remote control unit provides the user input for giving higher level commands such as the running speed, and turning direction, presently via a joystick.

Each leg is directly actuated by a Maxon RE118751 20W brushed DC motor combined with a Maxon 114473 two-stage 33:1 planetary gear [11], delivering an intermittent stall torque of 6 Nm. Even though each motor is PWM voltage controlled, additional back-EMF compensation in software permits approximate motor torque control. The motor angle, and thus the leg angles, are controlled via 1 kHz PD control loops. The software also features several safety measures, including fault detection for the encoders, estimation of the rotor temperatures to avoid motor damage, and a watchdog timer which disables the motors and resets the computer in case of software failures.

The main body measures 53x20x15 cm. The legs are made from 1 cm diameter Delrin rods and are "C" shaped to provide compliance primarily in the radial direction and permit easy clamping to the gear shaft. The leg length is 17.5 cm, measured as the vertical distance from ground to the gear shaft when standing

up. The encoder/motor/gear stacks protrude from the main body and the maximum widths of the front and back legs amount to 39.4 cm, measured at half the leg length. To provide clearance for the rotating front and back legs, the motors for the middle legs are further offset and result in a maximum width of 52 cm. The total mass of the robot is 7 kg with each leg contributing only approximately 10 g.

5.2 Experimental Results

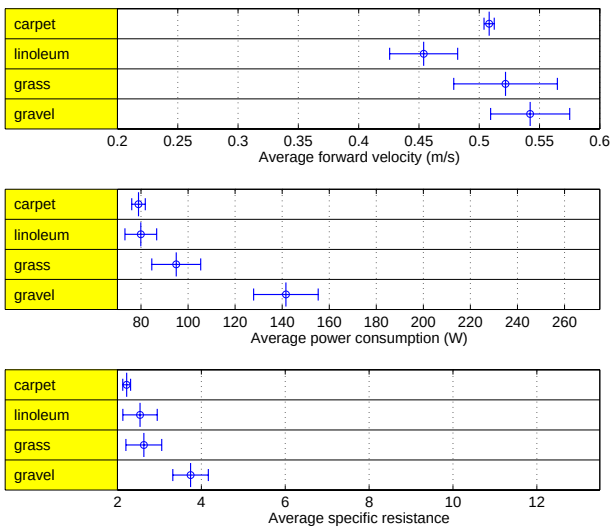

Figure 8: *Comparison of average forward velocity and energetics for different experiments.*

In this section, we report a set of experiments assessing the performance of our design on different types of terrain. In all of these settings, RHex is able to produce behavioral repertoire of Section 3, achieving stable and fast locomotion at speeds exceeding one body length per second.

Figure 8 summarizes the average forward running velocity and energetics for RHex while traversing carpet, Linoleum, grass and coarse gravel with the two-stroke open loop controller of Section 3. For these experiments, we ran the robot over carpet, linoleum, grass and gravel. The carpet and linoleum surfaces were standard office floors found close to the lab. For the outdoor surfaces, the grass was wet and showed height variations of about 2 cm. The gravel patch contained fairly large gravel pieces between three and eight cm diameter (see Figure 1).

For all the experiments, the robot was driven over a test stretch of 2 m. In order to obtain precise timing and to synchronize the data logging with the test stretch, a switch was mounted in the front of the robot, which was triggered as the robot ran into a Styrofoam panel held at the beginning and the end of the test stretch. The runs over each surface were repeated until ten successful runs were obtained. The average velocity and power consumption for each run was then computed with the available data. Moreover, to measure energy efficiency we used the "Specific Resistance" [9], $\varepsilon = P/(mgv)$, based on the robot's weight, mg, and its average power consumption, P, at a particular speed, v.

The robot moved well over these indoor and outdoor surfaces, with only minor velocity variations between 0.45 m/s and 0.55 m/s. The velocity on Linoleum was lowest due to intermittent slipping, which also causes a larger standard deviation of the runs compared to carpet. The surface irregularities of the outdoor grass and gravel surfaces provided improved traction, and therefore average velocities slightly above 0.5 m/s, but also resulted in larger variations between the runs. The specific resistance (power consumption) was lowest on carpet with 2.21 (80 W) and highest on gravel with 3.74 (140 W).

6 Conclusion

Nimble, robust locomotion over general terrain remains the sole province of animals, notwithstanding our functional prototype, RHex, nor the generally increased recent interest in legged robots. It is surely not evident from the RHex morphology, but our design and longer term controller development effort has been heavily influenced by considerations from biology. In particular, we believe that systematic application of certain operational principles exhibited by animals will achieve significant increases in RHex performance, and inform the evolution of the underlying mechanical design of future prototypes as well. To conclude the paper, we provide a brief sketch of these principles and how they may be applied.

Accumulating evidence in the biomechanics literature suggests that agile locomotion is organized in nature by recourse to a controlled bouncing gait wherein the "payload", the mass center, behaves mechanically as though it were riding on a pogo stick [3]. While Raibert's running machines were literally embodied pogo sticks, more utilitarian robotic devices such as RHex must actively anchor such templates within their alien morphology if the animals' capabilities are ever to be successfully engineered [8]. We have previously shown how to anchor a pogo stick template in the more related morphology of a four degree of freedom monopod [17]. The extension of this technique to the far more

distant hexapod morphology surely begins with the adoption of an alternating tripod gait, but its exact details remain an open question, and the minimalist RHex design (only six actuators for a six degree of freedom payload!) will likely entail additional compromises in its implementation. Moreover, the only well understood pogo stick is the Spring Loaded Inverted Pendulum [19], a two degree of freedom sagittal plane template that ignores body attitude and all lateral degrees of freedom. Recent evidence of a horizontal pogo stick in sprawled posture animal running [13] and subsequent analysis of a proposed lateral leg spring template to represent it [18] advance the prospects for developing a spatial pogo stick template in the near future. Much more effort remains before a functionally biomimetic six degree of freedom "payload" controller is available, but we believe that the present understanding of the sagittal plane can already be used to significantly increase RHex's running speed, and, as well, to endow our present prototype with an aerial phase.

Acknowledgements

This work was supported in part by DARPA/ONR Grant N00014-98-1-0747. Bob Full consulted on many of the design decisions and provided numerous tutorial explanations of the biomechanics literature. Noah Cowan offered very helpful advice concerning modeling and simulation. Liana Mitrea made invaluable contributions in the mechanical construction of the hexapod platform.

References

[1] R. J. Bachman, G. M. Nelson, W. C. Flannigan, R. D. Quinn, J. T. Watson, A. K. Tryba, and R. E. Ritzmann. Construction of a Cockroach-like hexapod robot. In *Eleventh VPI & SU Symposium on Structural Dynamics and Control*, pages 647–654, Blacksburg, VA, May 1997.

[2] R. D. Beer, H. Chiel, R. D. Quinn, and R. E. Ritzmann. Biorobotic Approaches to the Study of Motor Systems. *Current Opinion in Neurobiology*, 8:777–782, 1998.

[3] R. Blickhan and R. J. Full. Similarity in multilegged locomotion: bouncing like a monopode. *Journal of Comparative Physiology*, A. 173:509–517, 1993.

[4] R. A. Brooks. A Robot That Walks; Emergent Behaviors from a Carefully Evolved Network. Memo 1091, MIT AI Lab, February 1989.

[5] M. Buehler, R. Battagila, A. Cocosco, G. Hawker, J. Sarkis, and K. Yamazaki. SCOUT: A simple quadraped that walks, climbs and runs. In *Proceedings of the IEEE International Conference On Robotics and Automation*, pages 1707–1712, Leuven, Belgium, May 1998.

[6] M. Buehler, A. Cocosco, K. Yamazaki, and R. Battaglia. Stable open loop walking in quadruped robots with stick legs. In *Proceedings of the IEEE International Conference On Robotics and Automation*, Detroit, Michigan, May 1999.

[7] K. S. Espenscheid, R. D. Quinn, H. J. Chiel, and R. D. Beer. Biologically-Inspired Hexapod Robot Control. In *Proceedings of the 5th International Symposium on Robotics and Manufacturing: Research, Education and Applications (ISRAM' 94)*, Maui, Hawaii, August 1994.

[8] R. J. Full and D. E. Koditschek. Templates and Anchors: Neuromechanical Hypotheses of Legged Locomotion on Land. *Journal of Experimental Biology*, 202:3325–3332, 1999.

[9] G. Gabrielli and T. H. von Karman. What price speed? *Mechanical Engineering*, 72(10):775–781, 1950.

[10] P. C. Hughes. *Spacecraft Attitude Dynamics*. John Wiley & Sons, New York, 1986.

[11] Interelectric AG, Sachseln, Switzerland. *Maxon Motor Catalog*, 1997/98, www.maxon.com.

[12] ISRobotics. Autonomous Legged Underwater Vehicle. *http://www.isr.com/research/ariel.html*, 1999.

[13] T. M. Kubow and R. J. Full. The role of the mechanical system in control: A hypothesis of self-stabilization in hexapedal runners. *Phil. Trans. R. Soc. Lond.*, B. 354:849–862, 1999.

[14] G. M. Nelson and R. D. Quinn. Posture Control of a Cockroach-like Robot. In *Proceedings of the IEEE International Conference On Robotics and Automation*, pages 157–162, Leuven, Belgium, May 1998.

[15] M. H. Raibert. *Legged robots that balance*. MIT Press, Cambridge MA, 1986.

[16] U. Saranli. *SimSect Programmer's Manual*. The University of Michigan, 1999. In preparation.

[17] U. Saranli, W. J. Schwind, and D. E. Koditschek. Toward the Control of a Multi-Jointed, Monoped Runner. In *Proceedings of the IEEE International Conference On Robotics and Automation*, Leuven, Belgium, May 1998.

[18] J. Schmitt and P. Holmes. Mechanical models for insect locomotion I: Dynamics and stability in the horizontal plane. *Biological Cybernetics*, submitted, 1999.

[19] W. J. Schwind and D. E. Koditschek. Approximating the Stance Map of a 2 DOF Monoped Runner. *Journal of Nonlinear Science*, to appear.